Preprints of the 21st IFAC World Congress (Virtual)
Berlin, Germany, July 12-17, 2020

Design of a PI-Controller Based on Time-Domain Specification Utilizing the Parameter Space Approach

Eduard Popp *, **Mathias Tantau** *, **Mark Wielitzka** *, **Dennis Giebert** **, **Tobias Ortmaier** *

* *Leibniz University Hanover, Institute of Mechatronic Systems, An der Universität 1, 30823 Garbsen, Germany (e-mail: eduard.popp@imes.uni-hannover.de).*
** *IAV Automotive Engineering, Rockwellstraße 5, Germany.*

Abstract: In automotive application PI and PID controllers are widely used. Commonly the controller parametrization is performed in a heuristic manner in the vehicle at different operating points. Model-based approaches offer many advantages like a reduced effort of the design process and a more systematically investigation of the parameter set. Circumventing experiments at the vehicle is not feasible, however the goal is to achieve a significant reduction of this part of work. The aim of this paper is to find the controller parameter region, that ensures compliance with defined measures of the controller performance in time domain. On the basis of the parameter space approach these measures need to be transferred into the s-domain, which is shown exemplary for a second order system and a PI-controlled integrator system. The latter serves as a simple vehicle drive train model for the design of the engine idle speed controller.

Keywords: Automotive control, control system design, algebraic approaches, PI controller, performance analysis

1. INTRODUCTION

In automotive application PI and PID controllers are widely used considering for example the cruise control (Tiganasu et al. (2016)), lambda control or engine idle speed control (Guzzella and Onder (2010)). Commonly the controller parametrization is performed in a heuristic manner in the vehicle at different operating points. The adjustment stated in Schwarze et al. (2020) follows the Ziegler/Nichols or Chain/Horns/Roswick approach or meets a certain gain and phase margin in a nyquist chart respectively in a bode plot. The plant is typically assumed to be a first order system with time delay. These approaches are time consuming and don't take performance requirements into account, that arise from comfort demands of the customer. In an automotive application such specification are commonly formulated in time-domain like settling time and overshoot. In contrast, model-based approaches offer many advantages like a reduced effort of the design process and a more systematically investigation of the parameter set. Moreover, structural uncertainties can also be considered that arise from tolerances caused by ageing and manufacturing. Circumventing experiments at the vehicle is not feasible, however the goal is to achieve a significant reduction of this part of work. The objective of this paper is to develop a procedure in order to find an admissible region of control parameters that corresponds to time specification.

Regarding algebraic solutions, there are several approaches reported in the literature. One is based on the relation of the coefficients of the characteristic polynomial and settling time as well as the overshoot, that are claimed by Naslin (1969). The coefficient diagram method, introduced by Manabe (1998) and the characteristic ratio assignments developed by Kim et al. (2003), make use of this and propose a design technique that is based on the so-called characteristic ratios and the generalized time constant. The drawback of this approach is that a proper parameterization of these features with regard to the required performance measures cannot be given analytically. The assignments are obtained in Kim et al. (2003) by an iterative adjustment. A further comprehensive way is using the parameter space approach (PSA) introduced by Ackermann (2002). Given stability boundaries in s-space are mapped into a two dimensional parameter space. Ackermann (2002) discussed the relation between time performance measures and the position of the eigenvalues of the characteristic polynomial regarding a dominant pole pair. However an algebraic solution is not explicitly given in order to capture certain performance measures. Furthermore, it must be stated, that the step response is affected not only by poles but also zeros, hence it is not possible to carry out a generic solution for more complex systems. In case of higher order system with poles and zeros, these relations are valid only for certain conditions. Generally, it must be regarded more carefully. This paper focuses on finding accurate equivalent curves in s-plane in order to map time performances into controller parameter space using the PSA. The solution is obtained by applying the inverse Laplace transformation. A related work was done by Basilio and Matos (2002). Two types of systems are regarded in an exemplary way, that will bring to light differences and similarities. The aim is to derive design rules from the two exemplary analyzed systems, that can be applied on a vehicle drive train model.

This paper is organized as follows. In Section 2 a vehicle drive train is introduced. For design purpose a simplified model is considered. Afterwards this contribution gives a short overview of the PSA in Section 3, considering common stability boundary curves. Subsequently, equivalent curves for the overshoot and settling time are presented regarding a second order system and an integrator plant governed by a PI controller. In order to examine the accuracy of the proposed equivalent curves for the simplified drive train model, an equidistant distribution of the controller values is evaluated related to a priory defined performance specification. Finally a short outlook is given to discuss the capability for more complex systems. The paper ends up with a conclusion.

2. VEHICLE MODEL IN CLOSED LOOP

The proposed design method shall be applied on an engine idle speed controller of a vehicle in neutral gear. In order to apply the proposed method, a linear model is required. Taking the low-frequency dynamics into account, a simplified model can be derived from the drive train model that was introduced in Popp et al. (2019). For this purpose the following linear model with time delay is assumed:

$$\begin{aligned} J\dot{\omega}(t) &= T_{\mathrm{a}}(t - T_{\mathrm{D}}), \\ y(t) &= \tfrac{30}{\pi}\omega(t), \end{aligned} \tag{1}$$

where J is the total rotational mass, T_{a} is the applied torque less the amount of torque load acting on the crank shaft, y is the mean valued measured engine speed, ω the angular frequency of crank shaft and T_{D} the delay time. Out of the simplifications the following concerns arise to the design process:

(1) Regarding the transient step response of the reference value, an integrator plant is sufficient for a first controller design step as long as the controller values are limited to reasonable gains. Moreover, this is also a countermeasure to reduce high-frequency content of the actuator signal and in respect to amplification of sensor noise (see Ackermann (2002)).
(2) The objective of the controller design using a simplified model is to reduce the set of controller parameters to an admissible small region. Accordingly, explicit solutions for the performance specifications are required so that the subsequent controller design based on the nonlinear model incorporate the results as limiting conditions.

Considering a PI controller with the transfer function $C(s) = \frac{K_{\mathrm{p}}s+K_{\mathrm{i}}}{s}$ and for the plant $G_{\mathrm{veh}}(s) = \frac{30/\pi}{Js}e^{-sT_{\mathrm{D}}}$, the closed loop transfer function is:

$$F_{\mathrm{veh}}(s) = \frac{y(s)}{T_{\mathrm{a}}(s)} = \frac{\frac{K_{\mathrm{i}}}{J}(1+\frac{K_{\mathrm{p}}}{K_{\mathrm{i}}}s)\frac{30}{\pi}e^{-sT_{\mathrm{D}}}}{s^2 + (\frac{K_{\mathrm{p}}}{J}s + \frac{K_{\mathrm{i}}}{J})\frac{30}{\pi}e^{-sT_{\mathrm{D}}}}, \tag{2}$$

with controller parameters K_{p} and K_{i}. The delay time is approximated with pade of third order:

$$e^{-sT_{\mathrm{D}}} = \frac{-T_{\mathrm{D}}^3 s^3 + 12T_{\mathrm{D}}^2 s^2 - 60T_{\mathrm{D}}s + 120}{T_{\mathrm{D}}^3 s^3 + 12T_{\mathrm{D}}^2 s^2 + 60T_{\mathrm{D}}s + 120}. \tag{3}$$

3. PARAMETER SPACE APPROACH

On the basis of the given closed loop transfer function some performance requirements of the step response must be met by proper parameters of the PI controller. In order to utilize the PSA on the given performance requirements equivalent boundaries in the complex plane are defined. Finally these boundaries are mapped into the controller parameter space which is spanned by K_{p}-K_{i} axes. For this purpose a short introduction of the PSA is given. Regarding the characteristic polynomial of $F(s)$ the system is stable if its roots do not leave the left-half s-plane. Following the boundary crossing theorem by Frazer and Duncan (1929) the roots of this polynomial are continuous if the coefficients of the polynomial are continuous. This implies they cannot jump from the left-half s-plane to the right-half s-plane. Finding all roots of the polynomial that cross the imaginary boundary in dependence on some freely mapped parameters $\boldsymbol{q}$ reveals the boundaries of the stable region in parameter space. This concepts also holds for other boundary curves $\partial\Gamma$ in s-plane than the imaginary axis, e.g. negative real part or constant damping in case of further performance requirements of the system. A polynomial is called Γ-stable in Ackermann et al. (1991), if the roots are located in a prescribed region Γ in the s-plane. The Γ-region may consist of several composed curves $\partial\Gamma$. Crossing of eigenvalues over boundaries can occur in one of three ways: *real root boundaries* (RRB) at $s = 0$, *infinite root boundaries* (IRB) at $s = \infty$ and *complex root boundaries* (CRB) at $s = \sigma + j\omega$. More details can be found in Ackermann (2002).

3.1 Mapping $\partial\Gamma$-boundaries into parameter space

Consider a closed-loop system with an arbitary plant transfer function $G(s)$ and a controller $C(s)$ as introduced in Section 2. The transfer function of the closed-loop system and resulting characteristic polynomial is:

$$F(s) = \frac{G(s)C(s)}{1 + G(s)C(s)}, \tag{4}$$

$$P(s) = \mathrm{num}\{G(s)\}(K_{\mathrm{p}}s + K_{\mathrm{i}}) + \mathrm{den}\{G(s)\}s. \tag{5}$$

The main idea is to find a solution for each case:

$$\mathrm{RRB}: \quad P(s = 0, K_{\mathrm{p}}, K_{\mathrm{i}}) = 0 \tag{6}$$

$$\mathrm{CRB}: \quad P(s = \sigma + j\omega, K_{\mathrm{p}}, K_{\mathrm{i}}) = 0 \tag{7}$$

$$\mathrm{IRB}: \lim_{\omega\to\infty} P(s = \sigma + j\omega, K_{\mathrm{p}}, K_{\mathrm{i}}) = 0 \tag{8}$$

For the special case if $\partial\Gamma$ is described by the imaginary axis ($s = j\omega$) the idea is to leave ω as a parameter and calculate the control parameters by a sweep over ω, which is restricted to non-negative values. For the general case the boundary has to be described by a generalized parameter α that is analogously swept along the segments of $\partial\Gamma$. The formulation of this boundary is:

$$\partial\Gamma = \{s | s = \sigma(\alpha) + j\omega(\alpha), \alpha \in [\alpha^-; \alpha^+]\}. \tag{9}$$

So-called singular frequencies are not of our concern in this case, so they are not described here. Ackermann and Kaesbauer formulated in Ackermann (2002) a short notation for CRB mapping:

$$\begin{bmatrix} d_0(\alpha) & d_1(\alpha) & \cdots & d_n(\alpha) \\ 0 & d_0(\alpha) & \cdots & d_{n-1}(\alpha) \end{bmatrix} \boldsymbol{a}(\boldsymbol{q}) = \begin{bmatrix} 0 \\ 0 \end{bmatrix}, \quad (10)$$
$$\boldsymbol{D}(\alpha)\boldsymbol{a}(\boldsymbol{q}) = 0,$$

where

$$\begin{aligned} d_0(\alpha) &= 1 \\ d_1(\alpha) &= 2\sigma(\alpha) \quad (11) \\ d_{i+1}(\alpha) &= 2\sigma(\alpha)d_i(\alpha) - [\sigma^2(\alpha) + \omega^2(\alpha)]d_{i-1}(\alpha), \\ & \quad i = 1, 2, \ldots, n-1. \end{aligned}$$

$\boldsymbol{a}(\boldsymbol{q})$ is a parameter-depend coefficient function of the freely mapped parameters $\boldsymbol{q}$, while $\boldsymbol{D}(\alpha)$ is a description of $\partial\Gamma$. Solving this equation according to the control parameters represented in this contribution by $\boldsymbol{q} = [K_\mathrm{p}, K_\mathrm{i}]^\mathrm{T}$, yields the set of $\partial\Gamma$ in parameter space for each gridded value of α.

3.2 S-Domain Specification

In this Section common boundary curves are presented. Regarding a second order system the transfer function is

$$F(s) = \frac{\omega_0^2}{s^2 + 2\zeta\omega_0 s + \omega_0^2}. \quad (12)$$

According to Ackermann (2002) and Voßwinkel et al. (2019), a reasonable Γ-stable region in order to match time performance measures can be specified by:

(i) A damping ζ, which is bounded by a line with an angle to the imaginary axis. This curve corresponds to an equivalent overshoot. Consider, that the following remarks regard only the underdamped case, such that $\zeta \in [0, 1)$. An equivalent Γ-boundary for the overdamped case can be obtained analogously, but will not be covered by this proceeding.
(ii) A real part σ, which is bounded by a left-sided parallel to the imaginary axis. This curve corresponds to an equivalent settling time.
(iii) A bandwidth ω_0, which is bounded by a circular arc around the origin with radius R. This bound is needed to limit the control parameters to reasonable values.

In order to define the matrix $\boldsymbol{D}(\alpha)$, the curves need to be parameterized by the real part σ and the imaginary part ω of complex eigenvalues. Considering the equations

$$s = \sigma \pm j\omega = -\zeta\omega_0 \pm j\omega_e \quad (13)$$
$$\omega_0 = \sqrt{\sigma^2 + \omega^2}, \quad (14)$$
$$\zeta = \frac{-\sigma}{\sqrt{\sigma^2 + \omega^2}} \quad (15)$$
$$\omega_\mathrm{e} = \omega_0\sqrt{1 - \zeta^2} \quad (16)$$

the parameterization of the curves (i)-(iii) with respect to α can be obtained as follows:

$$\text{(i)}\ \omega = \sigma\frac{\sqrt{1 - \zeta_h^2}}{\zeta_h},\ \sigma = \alpha,\ \alpha \in [0, -\infty), \quad (17)$$
$$\text{(ii)}\ \omega^2 = \alpha,\ \sigma = \sigma_\varepsilon,\ \alpha \in [0, \infty), \quad (18)$$
$$\text{(iii)}\ \omega^2 = R^2 - \sigma^2,\ \sigma = \alpha,\ \alpha \in [-R, R]. \quad (19)$$

Using the symbolic toolbox the polynomial coefficients in $\boldsymbol{a}(\boldsymbol{q})$ are substituted with respect to the regarded system and $\boldsymbol{D}(\alpha)$ is composed according to (11). Finally the solution can be obtained by rewriting (10) after $K_\mathrm{p}(\alpha, t_\varepsilon, \varepsilon, h)$ and $K_\mathrm{i}(\alpha, t_\varepsilon, \varepsilon, h)$. In the following of this paper the use of h or ε as an index implies the proposed correspondence of the overshoot respectively the settling time to the variable.

4. EQUIVALENT TIME-DOMAIN SPECIFICATION

Finding an accurate equivalent represenation of performance measures according to (17)-(19) are required. In this context we want to find a parameterization of σ_ε as well as ζ_h and examine how suitable the proposed boundaries of Section 3.2 are. The following time-domain specifications are considered:

- A *settling time* $t_\varepsilon \leq t_{\varepsilon,\max}$ with a tolerance band of width 2ε and
- a *overshoot* $h \leq h_{\max}$.

The specification of performance requirements in s-domain is an indirect approach in order to meet time-domain demands. The step response depends primarily on the dominant pole, which has the smallest distance to the origin. In case further poles and zeros have less than twice the distance with respect to the dominant pole, these significantly affect the initial part of the step response. Thus, time specification cannot be satisfied by simple correspondences according to Section 3.1.

For an accurate mapping the time-domain specification have to be transformed into the s-domain according to the transfer function. To this end, the following method is pursued in this paper:

- Perform the inverse Laplace-transformation of the step response into time-domain.
- Formulate the requirements in time domain. Considering a unit step response it follows:

  Overshoot An overshoot can be described as:
  $$h = y(t_{\max}) - 1 = \mathcal{L}^{-1}\Big\{F(s)\frac{1}{s}\Big\}\Big|_{t=t_{\max}} - 1. \quad (20)$$
  The time of maximum overshoot $t_{\max}$ can be found by setting the derivation of $y(t)$ to zero:
  $$\frac{dy(t)}{dt} = \mathcal{L}^{-1}\{F(s)\} \stackrel{!}{=} 0. \quad (21)$$
  Settling time For the settling time t_ε considering a tolerance band of width 2ε it holds, that:
  $$\Big|y(t_\varepsilon) - 1\Big| = \Big|\mathcal{L}^{-1}\Big\{F(s)\frac{1}{s}\Big\} - 1\Big| \leq \varepsilon. \quad (22)$$
- Solve the equation for a suitable variable, that is the real part or the imaginary part of the pole.

In the following Section the method is applied to a second order system and PI controller with an integrator plant, that shall meet specified values of the above defined performance measures. The corresponding step responses to the given transfer functions $F(s)$ can be found e.g. in Lutz and Wendt (2019).

4.1 Second Order System

For the transfer function of a second order system the step response can be described as follows:

$$F(s) = \frac{\omega_0^2}{s^2 + 2\zeta\omega_0 s + \omega_0^2}, \quad (23)$$

$$y(t) = 1 - \frac{1}{\sqrt{1-\zeta^2}} e^{-\zeta\omega_0 t} \sin\Big(\omega_\mathrm{e} t + \arccos(\zeta)\Big) \quad (24)$$

Overshoot In order to find the maximum overshoot, time t_max is needed. Using equation (21) yields:

$$\frac{dy(t)}{dt} = \frac{\omega_0}{\sqrt{1-\zeta^2}} e^{-\zeta\omega_0 t_\mathrm{max}} \sin\Big(\omega_\mathrm{e} t_\mathrm{max}\Big) \overset{!}{=} 0, \quad (25)$$

$$\Rightarrow t_\mathrm{max} = \frac{\pi}{\omega_\mathrm{e}}. \quad (26)$$

Substituting t_max into equation (20) and neglecting the sine term yields:

$$e^{\frac{\sigma}{\omega_\mathrm{e}}\pi} = h \Rightarrow \omega = \sigma\frac{\pi}{\ln h}. \quad (27)$$

This equation can be rewritten with (15) such that an equivalent damping is obtained:

$$\zeta_h = \frac{-\sigma}{\sqrt{\sigma^2+\omega^2}} = \frac{1}{\sqrt{1+\left(\frac{\pi}{\ln h}\right)^2}}. \quad (28)$$

Settling time Next, the settling time is calculated. Consider the approach in (22) and use (24) leads to

$$-\frac{1}{\sqrt{1-\zeta^2}} e^{\zeta\omega_0 t_\varepsilon} = \varepsilon \quad (29)$$

by neglecting the sine term again. Solving this equation after $\sigma = -\zeta\omega_0$ yields:

$$\sigma = \frac{\ln(\varepsilon\sqrt{1-\zeta^2})}{t_\varepsilon} = \sigma_\varepsilon + \frac{\ln(\sqrt{1-\zeta^2})}{t_\varepsilon}, \quad (30)$$

with $\sigma_\varepsilon = \ln\varepsilon / t_\varepsilon$. According to the proposed correspondence of the settling time (18) a simple solution for the real part σ_ε is obtained. However this holds only for weakly damped second order systems. A precise curve can be found by solving (29) after ω. In the intermediate step

$$\zeta^2 = 1 - e^{2t_\varepsilon(\sigma-\sigma_\varepsilon)} \quad (31)$$

is substituted by (15) and yields:

$$\omega^2 = \sigma^2\frac{e^{2t_\varepsilon(\sigma-\sigma_\varepsilon)}}{1-e^{2t_\varepsilon(\sigma-\sigma_\varepsilon)}}. \quad (32)$$

Fig. 1 illustrates the boundaries in s-domain for a maximum overshoot and maximum settling time into a range of 2ε. Consider the real part σ_ε as characteristic feature.

4.2 PI-Controller with Integrator Plant

In this Section the procedure is applied to a PI-controlled integrator plant $G(s) = \frac{1}{Js}$. The step response can be described as follows:

$$F(s) = \frac{w_0^2(1+T_\mathrm{v}s)}{s^2+2\zeta\omega_0 s+\omega_0^2}, \quad (33)$$

$$\omega_0 = \sqrt{\frac{K_\mathrm{i}}{J}},\ \zeta = \frac{K_\mathrm{p}}{2\sqrt{K_\mathrm{i}J}},\ T_\mathrm{v} = \frac{K_\mathrm{p}}{K_\mathrm{i}} = \frac{2\zeta}{\omega_0},$$

$$y(t) = 1 - e^{-\zeta\omega_0 t}\Big(\cos(\omega_\mathrm{e}t) + \frac{\zeta - T_\mathrm{v}\omega_0}{\sqrt{1-\zeta^2}}\sin(\omega_\mathrm{e}t)\Big) \quad (34)$$

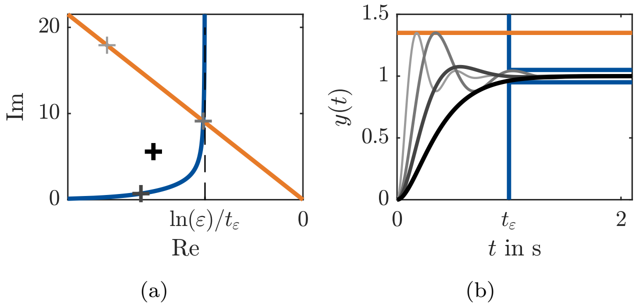

Fig. 1. PT$_2$-system: $\partial\Gamma$-boundaries of the overshoot $h = 0.35$ (orange line) and settling time $t_\varepsilon = 1s$ into a range of $\varepsilon = 0.05$ (blue line) and the corresponding step responses of samples on the combined boundary lines.

Overshoot Using (21) for calculating t_max the derivation $dy(t)/dt$ is:

$$\frac{dy(t)}{dt} = \omega_0 e^{-\zeta\omega_0 t}$$

$$\underbrace{\Big(T_\mathrm{v}\cos(\omega_\mathrm{e}t_\mathrm{max}) + \frac{1-\zeta T_\mathrm{v}\omega_0}{\omega_\mathrm{e}}\sin(\omega_e t_\mathrm{max})\Big)}_{\overset{!}{=}0} \overset{!}{=} 0 \quad (35)$$

$$\Rightarrow t_\mathrm{max} = \Big(\pi - \arctan\Big(\frac{-2\sigma\omega}{\sigma^2-\omega^2}\Big)\Big)\frac{1}{\omega}. \quad (36)$$

Using (20) and (21) yields:

$$h = -e^{\sigma t_\mathrm{max}}\underbrace{\Big(\cos(\omega t_\mathrm{max}) + \frac{\sigma}{\omega}\sin(\omega t_\mathrm{max})\Big)}_{=-1} \quad (37)$$

$$\Rightarrow \tan\Big(\ln(h)\frac{\omega}{\sigma}\Big) = \frac{-2\sigma\omega}{\sigma^2-\omega^2}. \quad (38)$$

A solution for ω of the nonlinear equation

$$f_1(\sigma,\omega) = \omega^2 - \frac{2\sigma\omega}{\mu} - \sigma^2 = 0, \quad (39)$$

with $\mu = \tan(\ln(h)\omega/\sigma)$ can be obtained by finding the roots by means of numeric optimization. The resulting boundary is likewise a straight line with constant damping, as shown in Fig. 2(a). However, an explicit solution for the equivalent damping cannot be given. The minimum overshoot is obtained for a maximum damping ratio of $\zeta = 1$ respectively $\omega \to 0$ and σ is fixed. In the opposite case $\zeta = 0$ is reached if $\sigma \to 0$ and ω is fixed. This leads to $h_\mathrm{min} > h > h_\mathrm{max}$:

$$\lim_{\omega\to 0}\tan\Big(\ln(h_\mathrm{min})\frac{\omega}{\sigma}\Big) = \ln(h_\mathrm{min})\frac{\omega}{\sigma} = \frac{-2\sigma\omega}{\sigma^2-\omega^2},$$

$$\Rightarrow h_\mathrm{min} = e^{-2}, \quad (40)$$

$$\lim_{\sigma\to 0}\frac{-2\sigma\omega}{\sigma^2-\omega^2} = 0 = \tan\Big(\ln(h_\mathrm{max})\frac{\omega}{\sigma}\Big),$$

$$\Rightarrow h_\mathrm{max} = e^0. \quad (41)$$

Settling time Using (14),(15) and (34) in (22) yields:

$$\Big|e^{\sigma t}\Big(\cos(\omega t) + \frac{\sigma}{\omega}\sin(\omega t)\Big)\Big| \le \varepsilon. \quad (42)$$

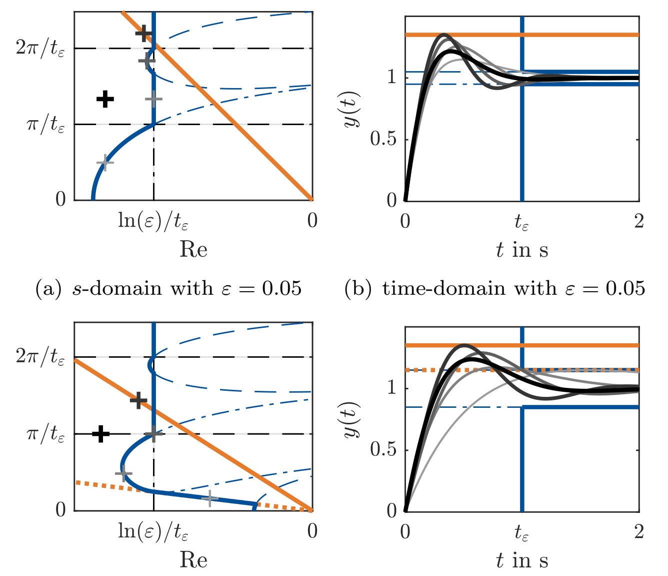

(a) s-domain with $\varepsilon = 0.05$ (b) time-domain with $\varepsilon = 0.05$

(c) s-domain with $\varepsilon = 0.15$ (d) time-domain with $\varepsilon = 0.15$

Fig. 2. PDT$_2$-system: $\partial\Gamma$-boundaries of the overshoot $h = 0.35$ (orange line) and settling time $t_\varepsilon = 1s$ into different ranges of ε (blue line) and the corresponding step responses of samples on the combined boundary lines.

In this case three solutions must be considered. The first solution is obtained by neglecting the trigonometric term in the brackets of $y(t)$, so that it holds:

$$\sigma = \frac{\ln(\varepsilon)}{t_\varepsilon} = \sigma_\varepsilon. \tag{43}$$

This is true if $|\sigma| \gg |\omega|$, such that $\cos(\omega t) + \frac{\sigma}{\omega}\sin(\omega t) < 1$. Otherwise the neglected term in (42) becomes critical. According to the upper bound $1+\varepsilon$ and the lower bound $1-\varepsilon$ a solution for both cases can be obtained by solving the implicit equation:

$$f_2(\sigma,\omega) = -\left|e^{\sigma t}\Big(\cos(\omega t) + \frac{\sigma}{\omega}\sin(\omega t)\Big)\right| \pm \varepsilon = 0, \tag{44}$$

Once again a numerical solver is used. The resulting curves are illustrated in Fig 2(a). Along the dashed line all step responses cross t_ε at $1+\varepsilon$ as shown in Fig 2(b). The dashed-dotted line corresponds to step responses that go through $y(t = t_\varepsilon) = 1 - \varepsilon$. In order to avoid, that the step responses leave the requested band width after once crossing the boundaries, the eigenvalues must lie on the left side of σ_e. In summary, the solid blue line is obtained, which is composed of all three solutions. Regarding the case $\varepsilon > h_{\min}$ as shown in Fig 2(c) and 2(d), the equivalent damping ratio of $h_{\min}$ must be also considered, which is pictured by the dashed line.

4.3 Mapping Rules

Comparing the results with the proposed correspondence from Section 3.2 similar results of the two systems are revealed. The overshoot complies with an equivalent damping. In terms of the settling time a real part must be taken into account as one of further limiting $\partial\Gamma$-boundaries. Unfortunately a solution for an explicit parameterization could not be found in Section 4.2.

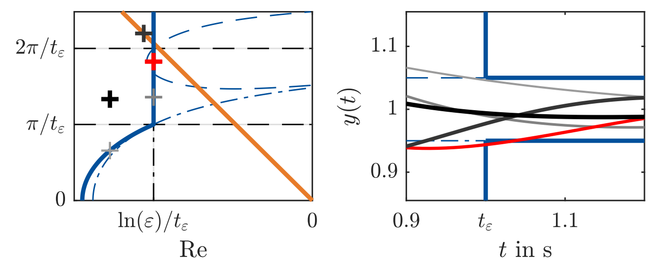

(a) s-domain using s^* for parameterization of $\partial\Gamma$. (b) time-domain using s^* for parameterization of $\partial\Gamma$.

Fig. 3. PDT$_2$-system: $\partial\Gamma$-boundaries of the overshoot $h = 0.05$ (orange line) and settling time $t_\varepsilon = 1s$ into different ranges of ε (blue line) and the corresponding step responses of samples on the combined boundary line.

In order to derive generic specifications, the prescribed concerns from Section 2 need to be responded. In order to limit the controller gains, a minimum overshoot shall be demanded. According to $\zeta \in [0,1)$, (28) and (40) , we propose $h_{\min} = 0$ in case of a second order system closed loop system respectively $h_{\min} = e^{-2}$ in case of an additional zero. Moreover, a lower limit of the settling time $t_{\varepsilon,\min}$ must also be introduced with respect to the limitation of controller gains. Responding to the second design concern an explicit solution of an equivalent $\partial\Gamma$ shall be derived in case of the PI-controlled integrator system. The results from Section 3.2 indicate that $\partial\Gamma$ concerning the settling time may be approximately composed of a real part and a circular arc. Considering the intersection point at the complex eigenvalues

$$s^* = \sigma^* + j\omega^*, \text{ with } \sigma^* = \frac{\ln(\varepsilon)}{t_\varepsilon},\ \omega^* = \frac{\pi}{t_\varepsilon} \tag{45}$$

yield proper parameterization of (18) and (19) as follows:

$$\sigma_\varepsilon = \sigma^*, \tag{46}$$

$$R_\varepsilon = \sqrt{(\sigma^*)^2 + (\omega^*)^2}, \tag{47}$$

which is shown in Fig. 3(a) and 3(b). In case of the lower limit of $t_{\varepsilon,\min}$ the corresponding real part curve must be omitted (compare to Fig. 4). The equivalent curve of the explicit simplification entails a slight violation of the criteria. Regarding the step response at the critical case pointed out in red, the process variable is about 0,6% beneath the lower boundary at t_ε. Typically, this error does not exceed 1%, varying the time-domain requirements. Concerning the overshoot yields:

$$\zeta_h = \frac{-\sigma}{\sqrt{\sigma^2 + \omega^2}} \tag{48}$$

evaluating $f_1(\sigma,\omega)$ in (39) in an assigned point.

5. RESULTS

In this Section the results will be applied on the simplified drive train model that was introduced in Section 2 with $J = 0.3\,\mathrm{kg\,m^2}$ and $T_\mathrm{D} = 0.03\,\mathrm{sec}$. First, the time-domain requirements on the controller design are presented, which are used to design a Γ-stable region in s-domain according to mapping rules from Section 4.3. The transformed region in parameter space using the PSA are shown in

4(b). As $K_\mathrm{p}(\alpha)$ and $K_\mathrm{i}(\alpha)$ are broken rational functions depending on α with order up to seven due to the pade-approximation, the functions are not explicitly stated. The enclosed Γ-region is validated by simulations in time-domain. With respect to a higher order system, finally the approach is examined based on a linear two-mass system coupled with a spring-damper element.

5.1 Performance Requirements

In order to verify the mapping and the lack of accuracy due to explicit parameterization, the closed loop of the vehicle model is designed following the presented methodology. For the PI-controller design a step size of $\Delta = 50\,\mathrm{min}^{-1}$ from $y = 780\,\mathrm{min}^{-1}$ to $y = 830\,\mathrm{min}^{-1}$ is assumed. The selected performance requirements with respect to a unit step response and the equivalent parameterization $\partial\Gamma$ are shown in Table 1. Applying these to the proposed step size of the reference value, the following specifications are obtained:

$$\begin{aligned}
&\text{Tolerance range}: && 827.50\,\mathrm{min}^{-1} < y < 832.50\,\mathrm{min}^{-1},\\
&\text{Settling time}: && 1\,\mathrm{s} < t_\varepsilon < 2\,\mathrm{s},\\
&\text{Peak}: && 836.75\,\mathrm{min}^{-1} < h < 847.5\,\mathrm{min}^{-1}.
\end{aligned}$$

Table 1. Performance requirements and equivalent Γ-specification

Requirement		Equivalent parameterization
$\Delta \cdot \varepsilon = 2.5\,\mathrm{min}^{-1}$,	$t_{\varepsilon,\max} = 2\,\mathrm{s}$	$R_{\min} = 2.170$ $\sigma_{\max} = -1.498$
$\Delta \cdot \varepsilon = 2.5\,\mathrm{min}^{-1}$,	$t_{\varepsilon,\min} = 1\,\mathrm{s}$	$R_{\max} = 4.34$
$h_{\max} = 35\%$		$\zeta_{\min} = 0.418$
$h_{\min} = 13.5\%$		$\zeta_{\max} = 1$

5.2 Controller Design for the Vehicle Model

The obtained Γ-stable region and its immediate neighborhood is explored by 900 simulated step responses, that are sampled from the gridded parameter space along equidistant distributed values. In this way each parameter set can be verified with respect to the time specifications and compared with Γ-stable region provided by the PSA. Fig. 4(b) illustrates the Γ-stable region in parameter space, that covers time-domain specification. Regarding the corresponding $\partial\Gamma$ curves in parameter space, there are two solutions: one represents the CRB and the other the RRB. Except of $\partial\Gamma$-boundary of the real part, the RRB lie on the K_p axis. The IRB does not exist. Comparing the results of the PSA and the evaluated gridded parameter sets, the region enclosed by $\partial\Gamma$ meets the requirements well, apart from a small border area. This is due to the curve simplification and the delay time. Valid parameter sets that are located outside the Γ-stable region, can be found along the CRB of $\zeta_{\max}$. In the given example a generally good coverage can be confirmed despite of the additional delay time.

5.3 Higher Order Systems

Consider the following plant:

$$G_\mathrm{dms}(s) = \frac{30/\pi}{(J_1+J_2)s}\,\frac{J_2 s^2 + ds + c}{\frac{J_1 J_2}{J_1+J_2}s^2 + ds + c}\,e^{-sT_\mathrm{D}} \tag{49}$$

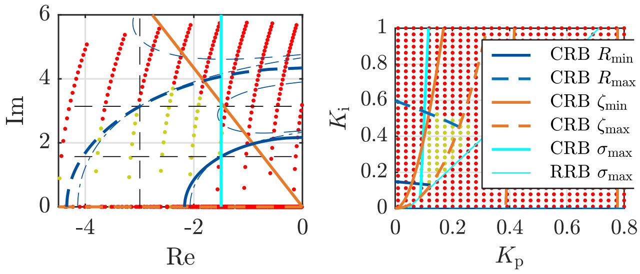

(a) Γ-stable region in s-domain (b) Corresponding region in parameter space

Fig. 4. The solid lines result from the maximum and dashed lines from the minimum requirements. Red colored dots represent gridded parameter sets, that violate the requirements. The opposing case is shown in green.

and its characteristic polynomial:

$$P_\mathrm{dms}(s) = \mathrm{num}\{G(s)\}(K_\mathrm{p}s + K_\mathrm{i}) + \mathrm{den}\{G(s)\}s. \tag{50}$$

Assuming $J = J_1 + J_2$ the two systems $G_\mathrm{dms}(s)$ and $G_\mathrm{veh}(s)$ show the same behaviour at lower frequencies as stated in Popp et al. (2019):

$$G_\mathrm{dms}(s \to 0) = \frac{30/\pi}{Js}. \tag{51}$$

Hence, it is conceivable, that the introduced Γ-region is also valid for this higher order system. However, due to the additional complex eigenvalue pair the region must be contracted by a further boundary. Despite the PSA is not limited to the analyzed models, it must be noticed that the mapping rules between time-domain and s-domain specification cannot be transferred. An analytic approach is not feasible in order to find an $\partial\Gamma$-boundary. A promising way is to assign an admissible damping ratio to the additional complex eigenvalue, such that the initial peak of the step response of $F_\mathrm{dms}(s)$ in reference to the step response of $F_\mathrm{veh}(s)$ decays into a requested band width ε_dms as illustrated in Fig 5(a). This can be obtained by simulating the step response with a set of K_p and K_i that is only about to meet the requirement with respect to ε_dms and $t_{\varepsilon,\mathrm{dms}}$. The corresponding damping ratio ζ_dms is either determined from the transfer function or is estimated from the measurement as follows:

$$n = \mathrm{floor}\Big(\frac{t_{\varepsilon,\mathrm{dms}} - t^*}{T_\mathrm{n}}\Big), \tag{52}$$

$$\Lambda = \frac{1}{n}\ln\Big(\frac{q^*}{\Delta\varepsilon_\mathrm{dms}}\Big), \tag{53}$$

$$\zeta_\mathrm{dms} = \frac{\Lambda}{\sqrt{4\pi^2 + \Lambda^2}}, \tag{54}$$

where T_n is the period time of one oscillation and q^* is the measured amplitude at the time t^*. The chart in Fig. 4(b) can be consulted for a proper choice of the control parameter values. Setting $J_1 = 0.18\,\mathrm{kg\,m}^2$, $J_2 = 0.12\,\mathrm{kg\,m}^2$, $c = 220\,\mathrm{Nm/rad}$ and $d = 0.2\,\mathrm{Nm/rad/s}$ a closed region in parameter space is obtained, that is shown in Fig. 5. In addition to the boundaries from Fig. 4(b) a further curve with equivalent damping ζ_dms is drawn, where $\boldsymbol{D}(\alpha)$ is parameterized according to (15) and $\boldsymbol{a}(\boldsymbol{q})$ contains the coefficients of the characteristic polynomial $P_\mathrm{dms}(s)$. In this case the band width ε_dms is identically

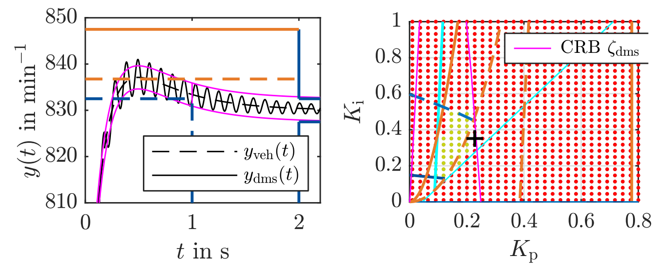

(a) step responses and time-domain specifications

(b) Corresponding region in parameter space

Fig. 5. Step responses of the vehicle model and higher order system in closed loop. The black marker in parameter space depicts the selected control parameters.

set to ε from Section 5.2 and $t_{\varepsilon,\mathrm{dms}}$ is equal to $t_{\varepsilon,\mathrm{min}}$. Nevertheless, it could also be set independently.

6. DISCUSSION

In this contribution an approach has been presented that associates the PSA directly with time-domain specifications. In the light of the results it becomes evident, that finding a satisfying region in respect to the requirements is possible. The proposed result is an accurate approximation. The derivation of equivalent $\partial\Gamma$-boundaries requires a complex calculation, that may provide implicit solutions as the simple vehicle model shows. Nevertheless, the two examined systems in comparison show similar curves of $\partial\Gamma$, that primarily differ in its parameterization. This especially turned out in case of the overshoot. Introducing e.g. a delay time or regarding a higher order plant ends up in more complex calculation in order to provide accurate solutions. However, in case of a moderate delay time, the deviation is still negligible. In case of more complex systems, the higher order dynamics can also be neglected in a first design step, as the low-frequency dynamic still rules the systems behaviour significantly. In a subsequent design step the complete system must be regarded. The PSA provides the stability boundary corresponding to $\sigma = 0$ for weak performance measures. Requesting a certain settling time as presented in Section 5.3 a corresponding damping ratio can be determined with respect to a critical step response. On this basis, it would be interesting to analyze further system as mentioned in view of achievable accuracy.

7. CONCLUSION

In any case, utilizating the PSA as controller design tool in automotive applications offers a direct relation between time-domain and s-domain. Thus, the boundaries can be parameterized on the basis of physically motivated performance measures. Summing up, the proposed method provides exact results in order to map a Γ-stable description in s-domain with performance measures in time-domain. An important result is, even-though considering the settling time only as a corresponding constant real part is not sufficient, composing $\partial\Gamma$ in addition with a circular arc provides an accurate solution. The given implicit boundaries are suitable for a graphical solution. An approximation by an explicit solution provides admissible results accepting some trade-off in the accuracy, but still an analytically description in parameter space is retained. Utilizing the PSA, further analyzes concerning e.g. robustness are viable.

REFERENCES

Ackermann, J. (2002). *Robust Control: the Parameter Space Approach*. Springer London.

Ackermann, J., Kaesbauer, D., and Muench, R. (1991). Robust gamma-stability analysis in a plant parameter space. *Automatica*.

Basilio, J.C. and Matos, S.R. (2002). Design of PI and PID controllers with transient performance specification. *IEEE Transactions on Education*.

Frazer, R.A. and Duncan, W.J. (1929). On the Criteria for the Stability of Small Motions. *Proceedings of the Royal Society A: Mathematical, Physical and Engineering Sciences*.

Guzzella, L. and Onder, C.H. (2010). *Introduction to modeling and control of internal combustion engine systems*. Springer.

Kim, K., Kim, Y., Keel, L., and Bhattacharyya, S. (2003). PID controller design with time response specifications. In *Proceedings of the 2003 American Control Conference, 2003*.

Lutz, H. and Wendt, W. (2019). *Taschenbuch der Regelungstechnik: mit MATLAB und Simulink*. Verlag Europa-Lehrmittel, Nourney, Vollmer GmbH & Company KG.

Manabe, S. (1998). Coefficient Diagram Method. *IFAC Proceedings Volumes*.

Naslin, P. (1969). *Essentials of Optimal Control*. Boston Technical Publishers.

Popp, E., Tantau, M., Wielitzka, M., Ortmaier, T., and Giebert, D. (2019). Frequency domain identification and identifiability analysis of a nonlinear vehicle drivetrain model. In *2019 18th European Control Conference (ECC)*.

Schwarze, K., Hinrichsen, C., Fein, O., Bucher, K., Projahn, U., Schaller, J., and Eckstein, C. (2020). *Elektronische Steuerung und Regelung*, 282–352. Springer Fachmedien Wiesbaden, Wiesbaden.

Tiganasu, A., Lazar, C., and Caruntu, C.F. (2016). Design and simulation evaluation of cooperative adaptive cruise control for a platoon of vehicles. In *2016 20th International Conference on System Theory, Control and Computing (ICSTCC)*.

Voßwinkel, R., Pyta, L., Schrödel, F., Mutlu, İ., Mihailescu-Stoica, D., and Bajcinca, N. (2019). Performance boundary mapping for continuous and discrete time linear systems. *Automatica*.